Inorg. Chem. **2007**, *46*, 2278–2285

Mechanistic Study of Iron(III) [Tetrakis(pentafluorophenyl)Porphyrin Triflate (F_{20}TPP)Fe(OTf) Catalyzed Cyclooctene Epoxidation by Hydrogen Peroxide

Ned A. Stephenson and Alexis T. Bell*

Chemical Sciences Division, Lawrence Berkeley Laboratory and Department of Chemical Engineering, University of California, Berkeley, California 94720-1462

Received May 4, 2006

We have recently proposed a mechanism for the epoxidation of cyclooctene by H_2O_2 catalyzed by iron(III) [tetrakis-(pentafluorophenyl)]porphyrin chloride, (F_{20}TPP)FeCl, in solvent containing methanol [Stephenson, N. A.; Bell, A.T. *Inorg. Chem.* **2006**, 45, 2758–2766]. In that study, we found that catalysis did not occur unless (F_{20}TPP)FeCl first dissociated, a process facilitated by the solvation of the Cl^- anion by methanol and the coordination of methanol to the (F_{20}TPP)Fe^+ cation. Methanol as well as other alcohols was also found to facilitate the heterolytic cleavage of the O–O bond of H_2O_2 coordinated to the (F_{20}TPP)Fe^+ cation via a generalized acid mechanism. In the present study, we have shown that catalytic activity of the (F_{20}TPP)Fe^+ cation can be achieved in aprotic solvent by displacing the tightly bound chloride anion with a weakly bound triflate anion. By working in an aprotic solvent, acetonitrile, it was possible to determine the rate of heterolytic O–O bond cleavage in coordinated H_2O_2 unaffected by the interaction of the peroxide with methanol. A mechanism is proposed for this system and is shown to be valid over a range of reaction conditions. The mechanisms for cyclooctene epoxidation and H_2O_2 decomposition for the aprotic and protic solvent systems are similar with the only difference being the mechanism of proton-transfer prior to heterolytic cleavage of the oxygen–oxygen bond of coordinated hydrogen peroxide. Comparison of the rate parameters indicates that the utilization of hydrogen peroxide for cyclooctene epoxidation is higher in a protic solvent than in an aprotic solvent and results in a smaller extent of porphyrin degradation due to free radical attack. It was also shown that water can coordinate to the iron porphyrin cation in aprotic systems resulting in catalyst deactivation; this effect was not observed when methanol was present, since methanol was found to displace all of the coordinated water.

Introduction

The peroxidase and catalase-like activity of iron porphyrins is well-known, and many studies have been devoted to elucidating the mechanism of porphyrin-catalyzed oxidation of alkanes and olefins.[1−57] These studies have revealed that the composition of the axial ligand and the composition of the solvent in which reactions are carried out have a strong effect on the catalytic activity of the porphyrin and the yield

* To whom correspondence should be addressed. E-mail: alexbell@berkeley.edu.

(1) Sheldon, R. A. *Metalloporphyrins in Catalytic Oxidations*; Marcel Dekker: New York, 1994.
(2) Montanari, F.; Casella, L. *Metalloporphyrins Catalyzed Oxidations;* Kluwer Academic Publishers: Boston, MA, 1994.
(3) Meunier, B. *Biomimetic Oxidations Catalyzed by Transition Metal Complexes;* Imperial College Press: London, 1999.
(4) Moore, K. T.; Horvath, I. T.; Therien, M. J. *Inorg. Chem.* **2000**, *39*, 3125−3139.
(5) Kalish, H. R.; Latos-Grazynski, L.; Balch, A. L. *J. Am. Chem. Soc.* **2000**, *122*, 12478−12486.
(6) Birnbaum, E. R.; Grinstaff, M. W.; Labinger, J. A.; Bercaw, J. E.; Gray, H. B. *J. Mol. Catal. A.: Chem.* **1995**, *104*, 119−122.
(7) Grinstaff, M. W.; Hill, M. G.; Birnbaum, E. R.; Schaefer, W. P.: Labinger, J. A.; Gray, H. B. *Inorg. Chem.* **1995**, *34*, 4896−902.
(8) Grinstaff, M. W.; Hill, M. G.; Labinger, J. A.; Gray, H. B. *Science* **1994**, *264*, 1311−1313.
(9) Mansuy, D. *Coord. Chem. Rev.* **1993**, *125*, 129−141.
(10) Balch, A. L. *Inorg. Chim. Acta* **1992**, *197*, 198−200.
(11) Meunier, B. *Chem. Rev.* **1992**, *92*, 1411−1456.
(12) Vaz, A. D. N.; Roberts, E. S.; Coon, M. J. *J. Am. Chem. Soc.* **1991**, *113*, 5886−5887.
(13) Bruice, T. C. *Acc. Chem. Res.* **1991**, *24*, 243−249.
(14) Traylor, T. G. *Pure Appl. Chem.* **1991**, *63*, 265−274.
(15) Gunter, M. J.; Turner, P. *Coord. Chem. Rev.* **1991**, *108*, 115−161.
(16) Ellis, P. E.; Lyons, J. E. *Coord. Chem. Rev.* **1990**, *105*, 181−193.
(17) Mansuy, D. *Pure Appl. Chem.* **1990**, *62*, 741−746.
(18) Wijesekera, T.; Matsumoto, A.; Dolphin, D.; Lexa, D. *Angew. Chem., Int. Ed.* **1990**, *29*, 1073−1074.
(19) Tsuchiya, S.; Seno, M. *Chem. Lett.* **1989**, 263−266.

10.1021/ic060757c CCC: $37.00
Published on Web 02/21/2007

of oxidation products relative to the consumption of hydrogen peroxide.[58−64] A system of particular interest has been the oxidation of olefins, such as cyclooctene, in which case the major, and sometimes even the exclusive, product is the epoxide. It has been shown for such systems that iron(III) porphyrins coordinated by a weakly bound axial ligand such as a triflate, perchlorate, hexafluoroantimonate, or nitrate anion are catalytically active in aprotic solvents (e.g., acetonitrile or methylene chloride) but that porphyrins coordinated by a strongly bound axial ligand such as a chloride or hydroxide anion are inactive in aprotic solvents.[60,61] However, when porphyrins coordinated by a strongly bound ligand are dissolved in a solvent containing a protic component, they become active.[62−66] Recent work in our laboratory with iron(III) [tetrakis(pentafluorophenyl)]-porphyrin chloride (F_{20}TPP)FeCl has shown that protic solvents enable the dissociation of (F_{20}TPP)FeCl as a consequence of their ability to solvate the Cl^- anion and coordinate to the (F_{20}TPP)Fe^+ cation.[64,65] Protic solvents have also been suggested to facilitate the heterolytic cleavage of porphyrin-coordinated H_2O_2 via generalized acid catalysis and thereby produce iron(IV) pi-radical cations that are active intermediates in the epoxidation of olefins.[62−65] While a consensus appears to have emerged about the qualitative effects of the axial ligand and solvent composition, the magnitude of these effects expressed in terms of the rate and equilibrium coefficients is only now beginning to be understood.

The aim of the present study was to elucidate the mechanism for epoxidation of cyclooctene using hydrogen peroxide as the oxidant and an iron porphyrin with a weakly coordinated ligand, (F_{20}TPP)Fe(OTf), dissolved in an aprotic solvent, acetonitrile, as the catalyst and to compare this mechanism to that which we have reported for the chloride-coordinated porphyrin in the presence of a protic solvent, methanol.[64,65] By working with a weakly coordinating ligand in an aprotic solvent it was possible to determine the rate parameters for the epoxidation of cyclooctene in the absence of the effects of a protic solvent acting as either a ligand to the iron porphyrin or as a cocatalyst in the heterolytic cleavage of the O−O bond of coordinated H_2O_2. A comparison was also undertaken of the rate parameters for the epoxidation of cyclooctene by H_2O_2 catalyzed by (F_{20}TPP)-Fe(OTf) and (F_{20}TPP)FeCl in methanol, to establish whether the catalytically active species in both cases is (F_{20}TPP)Fe-(CH_3OH)$^+$, as we have proposed previously.[64,65]

Experimental Procedures

Reagents. OmniSolv grade acetonitrile (99.99+%, water content 0.0022%), HPLC grade methanol (99.9+%), and ACS grade chloroform (99.8%) were obtained from EMD Chemicals. Iron-(III) [tetrakis(pentafluorophenyl)]porphyrin chloride, dodecane (99+%), ACS grade hydrogen peroxide (30 wt %), and silver trifluoromethanesulfonate (99.95+%) were obtained from Sigma Aldrich. *cis*-Cyclooctene (95%) was obtained from Alfa-Aesar. Deuterium oxide was obtained from Cambridge Isotope Laboratories, Inc. All chemicals were used without further purification or

(20) Montanari, F.; Banfi, S.; Quici, S. *Pure Appl. Chem.* **1989**, *61*, 1631−1636.
(21) Castellino, A. J.; Briuce, T. C. *J. Am. Chem. Soc.* **1988**, *110*, 158−162.
(22) Traylor, T. G.; Xu, F. *J. Am. Chem. Soc.* **1988**, *110*, 1953−1958.
(23) Groves, J. T.; Watanabe, Y. *J. Am. Chem. Soc.* **1988**, *110*, 8443−8452.
(24) Tabushi, I. *Coord. Chem. Rev.* **1988**, *86*, 1−42.
(25) Ostovic, D.; Bruice, T. C. *J. Am. Chem. Soc.* **1988**, *110*, 6906−6908.
(26) Castellino, A. J.; Bruice, T. C. *J. Am. Chem. Soc.* **1988**, *110*, 1313−1315.
(27) Traylor, T. G.; Nakano, T.; Mikzstal, A. R.; Dunlap, B. E. *J. Am. Chem. Soc.* **1987**, *109*, 3625−3632.
(28) Jorgensen, K. A. *J. Am. Chem. Soc.* **1987**, *109*, 698−705.
(29) Traylor, T. G.; Mikzstal, A. R. *J. Am. Chem. Soc.* **1987**, *109*, 2770−2774.
(30) Mansuy, D. *Pure Appl. Chem.* **1987**, *59*, 759−770.
(31) Groves, J. R.; Watanabe, Y. *J. Am. Chem. Soc.* ***1986***, *108*, *507−508.*
(32) Collman, J. P.; Kodadek, T.; Brauman, J. I. *J. Am. Chem. Soc.* **1986**, *108*, 2588−2594.
(33) Meunier, B. *Bull. Soc. Chim. Fr.* **1986**, *4*, 578−594.
(34) Bruice, T. C. *Ann. N. Y. Acad. Sci.* **1986**, *471*, 83−98.
(35) Traylor, T. G.; Nakano, T.; Dunlap, B. E.; Traylor, P. S.; Dolphin, D. *J. Am. Chem. Soc.* **1986**, *108*, 2782−2784.
(36) Groves, J. T.; Watanabe, Y. *J. Am. Chem. Soc.* **1986**, *108*, 507−508.
(37) Collman, J. P.; Kodadek, T.; Raybuck, S. A.; Brauman, J. I.; Papzian, L. M. *J. Am. Chem. Soc.* **1985**, *107*, 4343−4345.
(38) Traylor, T. G.; Marsters, J. C.; Nakano, T.; Dunlap, B. E. *J. Am. Chem. Soc.* **1985**, *107*, 5537−5539.
(39) Collman, J. P.; Brauman, J. I.; Meunier, B.; Hayashi, T.; Kodadek, T.; Raybuck, S. A. *J. Am. Chem. Soc.* **1985**, *107*, 2000−2005.
(40) Guengerich, F. P.; MacDonald, T. L. *Acc. Chem. Res.* **1984**, *17*, 9−16.
(41) Collman, J. P.; Brauman, J. I.; Meunier, B.; Raybuck, S. A.; Kodadek, T. *Proc. Natl. Acad. Sci. U.S.A.* **1984**, *81*, 3245−3248.
(42) Razenberg, J. A. S. J.; Nolte, R. J. M.; Drenth, W. *Tetrahedron Lett.* **1984**, *25*, 789−792.
(43) Mansuy, D.; Battioni, P.; Renaud, J. P. *J. Chem. Soc., Chem. Commun.* **1984**, 1255−1257.
(44) Traylor, T. G.; Lee, W. A.; Stynes, D. V. *J. Am. Chem. Soc.* **1984**, *106*, 755−764.
(45) Traylor, P. S.; Dolphin, D.; Traylor, T. G. *J. Chem. Soc., Chem. Commun.* **1984**, 279−280.
(46) La Mar, G. N.; De Ropp, J. S.; Latos-Grazynski, L.; Balch, A. L.; Johnson, R. B.; Smith, K. M.; Parish, D. W.; Cheng, R. J. *J. Am. Chem. Soc.* **1983**, *105*, 782−787.
(47) Ortiz de Monteallano, P. R.; Mangold, B. L. K.; Wheeler, C.; Kunze, K. L.; Reich, N. O. *J. Biol. Chem.* **1983**, *258*, 4208−4213.
(48) Collman, J. P.; Kodadke, T.; Raybuck, S. A.; Meunier, B. *Proc. Natl. Acad. Sci. U.S.A.* **1983**, *80*, 7039−7041.
(49) Groves, J. T.; Myers, R. S. *J. Am. Chem. Soc.* **1983**, *105*, 5791−5796.
(50) Groves, J. T.; Haushalter, R. C.; Nakamura, M.; Naemo, T. E.; Evans, B. J. *J. Am. Chem. Soc.* **1981**, *103*, 2884−2886.
(51) Mansuy, D.; Chottard, J. C.; Lange, M.; Battioni, J. P. *J. Mol. Catal.* **1980**, *7*, 215−226.
(52) Groves, J. T.; Nemo, T. E.; Myers, R. S. *J. Am. Chem. Soc.* **1979**, *101*, 1032−1033.
(53) Lowe, G. H.; Kert, C. J.; Hjelmeland, L. M.; Kirchner, R. F. *J. Am. Chem. Soc.* **1977**, *99*, 3534−3536.
(54) Nordblum, G. D.; White, R. E.; Coon, M. J. *Arch. Biochem. Biophys.* **1976**, *175*, 524−533.
(55) Dunford, H. B.; Stillman, J. S. *Coord. Chem. Rev.* **1976**, *19*, 187−251.
(56) Hrycay, E. G.; Gustafsson, J. A.; Ingelman-Sundberg, M.; Ernster, L. *Biochem. Biophys. Res. Commun.* **1975**, *66*, 209−216.
(57) Lichtenberger, F.; Nastaincyzk, W.; Ullrich, V. *Biochem. Biophys. Res. Commun.* **1975**, *70*, 939−946.
(58) Traylor, T. G.; Popovitz-Biro, R. *J. Am. Chem. Soc.* **1988**, *110*, 239−243.
(59) Lee, K. A.; Nam, W. *J. Am. Chem. Soc.* **1997**, *119*, 1916−1922.
(60) Nam, W.; Jin, S. W.; Lim, M. H.; Ryu, J. Y.; Kim, C. *Inorg. Chem.* **2002**, *41*, 3647−3652.
(61) Nam, W.; Lim, M. H.; Oh, S. Y.; Lee, J. H.; Lee, H. J.; Woo, S. K.; Kim, C.; Shin, W. *Angew. Chem., Int. Ed.* **2000**, *39*, 3646−3649.
(62) Nam, W.; Oh, S. Y.; Sun, Y. J.; Kim, J.; Kim, W. K.; Woo, S. K.; Shin, W. *J. Org. Chem.* **2003**, *68*, 7903−7906.
(63) Traylor, T. G.; Xu, F. *J. Am. Chem. Soc.* **1990**, *112*, 178−186.
(64) Stephenson, N. A.; Bell, A. T. *Inorg. Chem.* **2006**, *45*, 2758−2766.
(65) Stephenson, N. A.; Bell, A. T. *J. Am. Chem. Soc.* **2005**, *127*, 8635−8643.
(66) Stephenson, N. A.; Bell, A. T. *Inorg. Chem.* **2006**, *45*, 5591−5599.

drying. As discussed below, water can coordinate to the iron(III) porphyrin cations resulting in catalyst deactivation when only acetonitrile is present. However, further drying of acetonitrile was deemed unnecessary, since the acetonitrile, as received, contained only 0.0022% water, based on Karl Fischer analysis. This concentration of water is 2 orders of magnitude less than that added with 30 (w/w)% aqueous H_2O_2 under experimental conditions.

Synthesis of (F_{20}TPP)Fe(OTf). Triflate-coordinated porphyrin was synthesized based on the procedure of Nam et al.[67] Silver triflate (19.3 mg) was added to a magnetically stirred solution of (F_{20}TPP)FeCl (70 mg) dissolved in acetonitrile (7 mL). Conversion of the porphyrin from the chloride-coordinated form to the triflate-coordinated form was evidenced via ^{1}H NMR by a shift in the position of the β-pyrrole proton resonance from 81 to 60 ppm. The initial addition of silver triflate (~1 equiv based on porphyrin) resulted in no change in coordination. Approximately four additional equiv of silver triflate (77 mg) were then added, and the mixture was stirred for 24 h. Triflate coordination was then evidenced by the formation of a white precipitate (silver chloride) and the appearance of a broadened ^{1}H NMR peak at 60 ppm. Integration of this peak indicated that approximately 75% of the chloride ligand had been exchanged. Additional equiv of silver triflate were added incrementally allowing 12−24 h between each addition. After the addition of ~10.5 total equiv, ^{1}H NMR indicated that 96% of the chloride anions had been replaced by triflate anions. The white precipitate was then filtered from the reaction mixture, and two additional equiv of silver triflate (34 mg) were added to the porphyrin solution. The solution was filtered again, and ^{1}H NMR indicated that an additional 1% of the chloride anions had been replaced by triflate anions. ^{19}F NMR analysis of the porphyrin solution revealed three resonances attributed to the fluorine substituents on the phenyl groups attached to the porphyrin ring and one resonance attributed to the triflate anions. These features are located at −134.6 ppm, −152.2 ppm, and −160.1 ppm for the fluorine atoms located at the ortho-, para-, and meta-positions on the phenyl groups and at −77.1 ppm for the fluorine atoms associated with the triflate anions. Comparison of the areas for the peaks attributed to phenyl fluorine atoms to the area of the peak attributed to the fluorine atoms of the triflate anions indicated that the concentration of the triflate anions was an order of magnitude greater than that of the porphyrin. Since only a single ^{19}F NMR peak for triflate anions was observed at a position identical to that for free triflate anions, it is believed that all of triflate anions behave as free anions or weakly bound, outer-sphere ligands associated with the porphyrin cations.

Reactions. To investigate the epoxidation of cyclooctene, catalyst, solvent, cyclooctene, and dodecane, as an internal standard, were combined in a 5-mL glass vial with magnetic stirring. The solvent consisted of pure acetonitrile unless stated otherwise. The cyclooctene, porphyrin, and hydrogen peroxide concentrations were varied depending upon the experiment; however, the total reaction volume was always 3.34 mL. Hydrogen peroxide (1−10 μL) was added via a syringe to initiate the reactions. Reaction products were analyzed by injecting a 0.5 μL sample of the reaction mixture into an HP6890 series gas chromatograph fitted with an Agilent DB Wax (30 m × 0.32 mm × 0.5 μm) capillary column and an FID detector. The temperature program used for this analysis was as follows: hold for 2.5 min at 50 °C, ramp at 20 °C/min to 175 °C, and hold for 1.5 min at 175 °C. The split/splitless inlet was operated at 200 °C and 14.2 psi with a split ratio of 5. Dodecane (an internal standard) and cyclooctene epoxide were eluted at 5.5 and 8.2 min, respectively. The accuracy of measuring the epoxide concentration via gas chromatography was ±1% based on the analysis of a calibrated standard. Blank reactions were carried out without porphyrin catalyst present but with silver triflate present; these experiments showed that the silver cations do not contribute significantly to peroxide consumption.

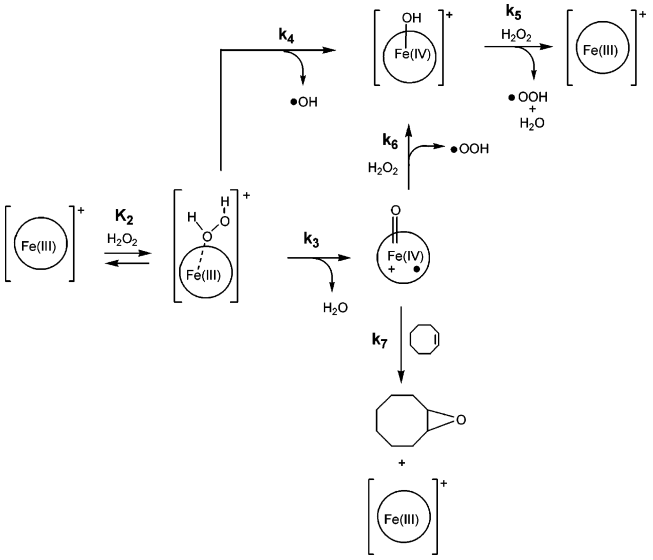

Figure 1. Proposed mechanism for the epoxidation of cyclooctene by H_2O_2 catalyzed by (F_{20}TPP)Fe(OTf).

NMR Spectroscopy. ^{1}H NMR was used to measure the concentration of hydrogen peroxide in situ as a function of time and to characterize the synthesized porphyrin. All experiments were performed at room-temperature 22 °C; the temperature varied by no more than ±0.1 °C as measured via a thermocouple located 2 mm from the NMR sample tube. All experiments used a 400 MHz Bruker VMX spectrometer. A detailed explanation of both procedures can be found elsewhere.[66,68]

UV−Visible Spectroscopy. UV−visible spectroscopy was used to characterize the axial coordination and oxidation state of the porphyrin in situ under reaction conditions. Absorbance experiments were conducted using a Varian Cary 400 Bio UV−visible spectrometer. The systematic error associated with UV−visible scans was negligible. Reactions with hydrogen peroxide were studied in situ by taking scans approximately every minute over the course of 20−30 min after the addition of hydrogen peroxide. Hydrogen peroxide (1 μL) was added to 3.34 mL of a reaction mixture containing (F_{20}TPP)Fe(OTf) (15 μM) and cyclooctene (0.14 M) dissolved in acetonitrile. For reactions without substrate present, additional acetonitrile was substituted for the cyclooctene to maintain a constant reaction volume. Axial coordination of water was studied by taking UV−visible scans after the addition of 0.5 μL aliquots of water (up to 10 μL total) to (F_{20}TPP)Fe(OTf) (15 μM) dissolved in 3.34 mL of acetonitrile.

Reaction Mechanism. Nam and co-workers have presented convincing evidence that the (F_{20}TPP)Fe(OTf) catalyzed reaction with hydrogen peroxide as the oxidant results in the formation of pi-radical cation species as active intermediates for epoxidation.[60] Based on this information and our previous work,[64,65] the reaction mechanism shown in Figure 1 is postulated. (To facilitate comparison, the reaction numbering sequence used here is identical to that used in our earlier work with (F_{20}TPP)FeCl.[64,65]) In this

(67) Nam, W.; Lim, M. H.; Lee, H. J.; Kim, C. *J. Am. Chem. Soc.* **2000**, *122*, 6641−6647.

(68) Stephenson, N. A.; Bell, A. T. *Anal. Bioanal. Chem.* **2005**, *381*, 1289−1293.

mechanism, iron(III) porphyrin cations react reversibly with H_2O_2. The equilibrium constant for this reaction is K_2. The coordinated H_2O_2 then participates in reaction 3, as suggested by Nam and coworkers,[60] to produce the pi-radical cations and water via heterolytic cleavage of the oxygen−oxygen bond of hydrogen peroxide coordinated to (F_{20}TPP)Fe^+. In this process, the proton on the proximal oxygen is believed to be transferred to the distal oxygen by intramolecular rearrangement (see below). The oxygen−oxygen bond may also be cleaved homolytically via reaction 4 to produce an iron(IV) porphyrin species; this pathway results exclusively in the decomposition of hydrogen peroxide. In addition to being active for epoxidation via reaction 7, the pi-radical cations can also contribute to peroxide decomposition via reaction 6. However, this competitive pathway is minimal at high substrate concentrations.[64,65] Iron(IV) species generated by either reaction 4 or 6 are regenerated to the iron(III) state by reaction with additional H_2O_2, reaction 5. The hydroperoxyl radicals generated in reactions 5 and 6 react further to produce molecular oxygen,[69] while the hydroxyl radicals generated via reaction 4 are believed to contribute to oxidative degradation of the porphyrin ring.[65,70]

The observed rate constant for peroxide decomposition, k_{obs}, can be expressed according to eq 1. Pseudo-steady-state is assumed for the iron(IV) pi-radical cation species based on reaction 3 being the rate determining step. Here Y_∞ is the final yield of epoxide based on the overall consumption of H_2O_2, the limiting reagent, [(F_{20}TPP)Fe^+] is the concentration of iron(III) porphyrin cations, and k_3K_2 is defined according to the mechanism shown in Figure 1. Y_∞ can also be expressed in terms of the rate constants for homolytic and heterolytic cleavage, eq 2. Derivations of k_{obs} and Y_∞ are given elsewhere.[64,65]

$$k_{obs} = \frac{k_3K_2[(F_{20}TPP)Fe^+]}{Y_\infty} \quad (1)$$

$$Y_\infty = \frac{[\text{epoxide}]}{[H_2O_2]_0} \cong \frac{k_3}{k_3 + 2k_4} \quad (2)$$

Results and Discussion

Effects of Oxidant Concentration. In our previous studies of the mechanism of cyclooctene epoxidation by H_2O_2 catalyzed by (F_{20}TPP)Fe^+, we noted that both k_{obs} and Y_∞ are independent of the initial hydrogen peroxide concentration when the concentration of cyclooctene is sufficiently high that the rate of reaction 6 is small relative to the rate of reaction 7 (see Figure 1).[64,65] Based on the mechanism shown in Figure 1, both of these findings were also expected for the current porphyrin system. However, as shown in Figure 2, while Y_∞ is independent of the initial hydrogen peroxide concentration, $[H_2O_2]_0$, k_{obs} decreases monotonically with increasing $[H_2O_2]_0$. Since hydrogen peroxide was added to the system as a 30 (wt/wt)% aqueous solution, either water or hydrogen peroxide could be responsible for the observed behavior of k_{obs} with $[H_2O_2]_0$. The independence of Y_∞ on the oxidant concentration suggests that the cause for the decrease in k_{obs} occurs prior to reactions 3 and 4. To determine whether water or hydrogen peroxide was responsible for the change in the observed rate constant, deionized water was added to the reaction mixture prior to the addition of hydrogen peroxide. The results of this experiment are shown in Figure 3, where k_{obs} is plotted as a function of the water concentration. The diamond shaped data points connected by a solid line were obtained by varying the initial concentration of hydrogen peroxide, and the circular data points were obtained by holding the initial hydrogen peroxide concentration constant and adding water. The coincidence of the two sets of data indicates that k_{obs} is independent of the initial concentration of H_2O_2 but decreases with increasing concentration of water.

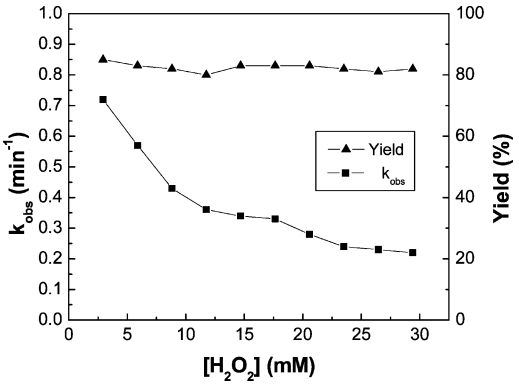

Figure 2. The effect of hydrogen peroxide concentration on the yield and observed rate constant. Porphyrin and substrate concentrations were 150 μM and 0.72 M, respectively.

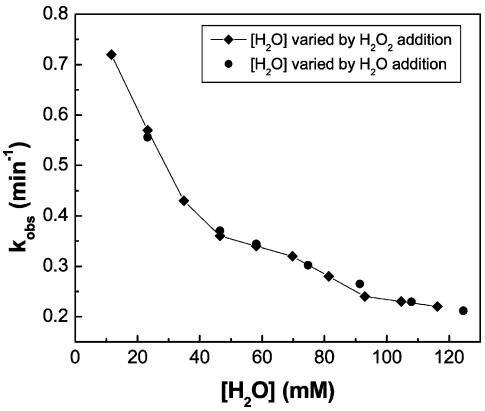

Figure 3. The effect of water concentration on the observed rate constant. The water concentration was varied both by changing the amount of H_2O_2 added and by direct addition of water. Porphyrin and substrate concentrations were 150 μM and 0.72 M, respectively. Hydrogen peroxide concentration was 2.9 mM for the experiments in which the concentration of H_2O was varied.

A possible cause for the decrease in the reaction rate with increasing water concentration is that water binds to the iron(III) porphyrin cation as an axial ligand resulting in a species that does not participate in catalysis. To investigate this possibility, porphyrin samples with different water concentrations were analyzed by UV−visible spectroscopy. In the absence of water, the iron(III) porphyrin cations were characterized by a Soret peak at 390 nm. As shown in Figure 4, the addition of water to the porphyrin solution resulted in a decrease in the absorbance at 390 nm, the formation of a shoulder on the Soret peak, and the formation of a new peak near 565 nm. Isosbestic points were seen at 405, 505, and 537 nm. We suggest that these changes in the absorption

(69) Nam, W.; Han, H. J.; Oh, S. Y.; Lee, Y. J.; Han, S. Y.; Kim, C.; Woo, S. K.; Shin, W. *J. Am. Chem. Soc.* **2000**, *122*, 8677−8684.
(70) Cunningham, I. D.; Danks, T. N.; Hay, J. N.; Hamerton, I.; Gunathilagan, S. *Tetrahedron* **2001**, *57*, 6847−6853.

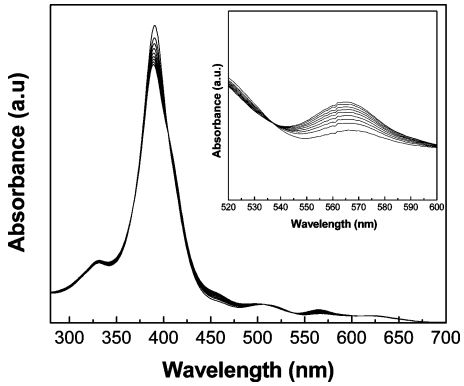

Figure 4. The effect of water on the UV−visible absorption spectrum. The porphyrin concentration was 15 μM, while the concentration of added water was varied from 0 to 166 mM.

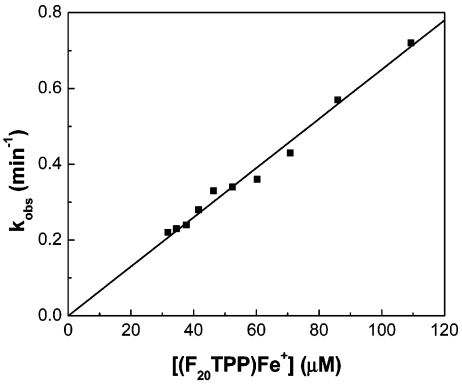

Figure 5. The observed rate constant versus [$(F_{20}TPP)Fe^+$] determined as a function of water concentration (12−116 mM).

spectrum were due to the coordination of water to the iron(III) porphyrin cations.

Water is thought to interact with the porphyrin cation as shown in eq 3. The porphyrin cation is likely coordinated by acetonitrile prior to coordination by water, and the resulting species after water coordination is likely six-coordinated with either one water molecule and one acetonitrile or two water molecules occupying the axial positions. However, the analysis discussed below is unaffected by initial coordination by acetonitrile, since the concentration of acetonitrile is large and essentially constant.

$$[(F_{20}TPP)Fe^+] + H_2O \overset{K_w}{\rightleftharpoons} [(F_{20}TPP)Fe(H_2O)^+] \quad (3)$$

Based on eq 3 and the change in absorbance at 565 nm, the value of K_w was determined to be 33 ± 6 M^{-1}. To determine whether eq 3 fully explains the nonlinear decrease in reaction rate, the concentrations of water-coordinated and free porphyrin cations were calculated, based on the above relationship, for the reaction conditions shown in Figure 2. As shown in Figure 5, the observed rate of reaction increases linearly with the concentration of free porphyrin cations, supporting the hypothesis that water-coordinated species are catalytically inactive. From the slope of the line in Figure 5, k_3K_2 is determined to be 90 ± 10 s^{-1} M^{-1}, and k_4K_2 is determined to be 9 ± 1 s^{-1} M^{-1} from eq 2. The relationship shown in eq 3 was also tested by varying the total porphyrin concentration. This also resulted in a linear correlation, not

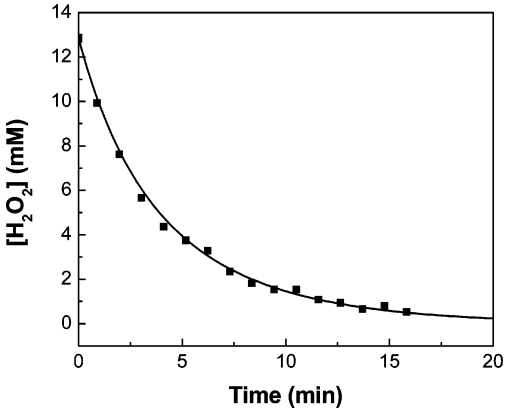

Figure 6. Variation in [H_2O_2] with time in the presence of cyclooctene. The data points are [H_2O_2] measured via ^{1}H NMR, and the solid line is [H_2O_2] predicted by the proposed mechanism. The total porphyrin concentration was ∼150 μM, and the cyclooctene concentration was ∼0.72 M.

shown, between the observed rate constant and the concentration of free iron(III) porphyrin cations. Based on the slope obtained from this analysis, k_3K_2 was found to be 82 ± 8 s^{-1} M^{-1}, and k_4K_2 was equal to 8 ± 1 s^{-1} M^{-1} based on eq 2. The final yield of epoxide was not affected significantly by the porphyrin concentration.

The mechanism by which water inhibits the catalytic activity of $(F_{20}TPP)Fe^+$ is not understood, and experiments to gather further insight into this phenomenon were not undertaken as a part of the present study. One possibility is that the water-coordinated porphyrin species form μ-oxo dimers, which are well-known to be catalytically inactive for the oxidation of organic substrates.[1,2] This interpretation may also explain why water deactivates the porphyrin catalyst while methanol does not. For two porphyrin species to dimerize, the individual iron cations must be able to approach each other to react. The alkyl group of a methanol molecule coordinated to the iron(III) cation may provide sufficient steric hindrance to inhibit the formation of μ-oxo dimers.

Consumption of Hydrogen Peroxide. The value of k_{obs} and the values of k_3K_2 and k_4K_2 reported above are based solely on the measured rate of cyclooctene epoxide formation. As a further test of the reaction kinetics, the actual rate of hydrogen peroxide consumption was measured by ^{1}H NMR. As shown in Figure 6, the temporal variation in the concentration of H_2O_2 is described accurately by the mechanism shown in Figure 1, and the rate parameters were determined from measurements of the initial rate of cyclooctene epoxidation. A value of k_5 = 225 M^{-1} s^{-1} was assumed, based upon previous studies of the kinetics for $(F_{20}TPP)FeCl$.[64,65] The validity of this assumption is discussed below.

The rate of peroxide consumption in the absence of cyclooctene was also determined by ^{1}H NMR. As shown in Figure 7, the consumption of hydrogen peroxide proceeds as predicted by the proposed mechanism and the rate parameters derived from the previous experiments with cyclooctene present. Furthermore, the predicted rate of peroxide decomposition in the absence of cyclooctene is very sensitive to the rate parameter k_5. This is due to the fact that

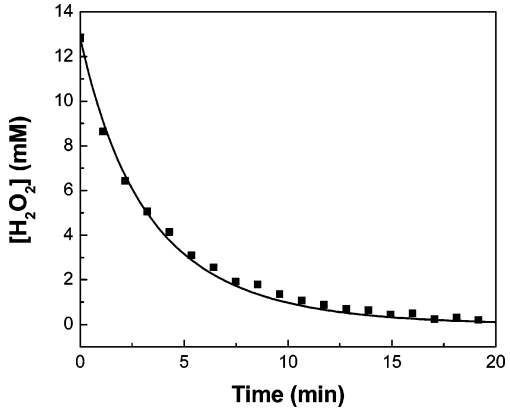

Figure 7. Variation in $[H_2O_2]$ with time in the absence of cyclooctene. Data points are $[H_2O_2]$ measured via ^{1}H NMR, and the solid line is $[H_2O_2]$ predicted by the proposed mechanism. The total porphyrin concentration was ~75 μM.

more than one-third of the peroxide is consumed via reaction 5 when cyclooctene is not present. The excellent agreement between the NMR data and the kinetic model validates the choice of 225 M^{-1} s^{-1} for k_5 and indicates that the rate coefficient for this reaction step is independent of the composition of the axial ligand associated with the porphyrin.

Formation of Iron(IV) Species. As shown above, the proposed model for the reaction kinetics accurately predicts the rates of hydrogen peroxide consumption both in the presence and absence of cyclooctene. The predictions of the model also agree qualitatively with observations made by UV−visible spectroscopy. The porphyrin reaction mixture was analyzed as a function of time after the addition of hydrogen peroxide both with and without cyclooctene present in order to establish evidence for the formation of iron(IV) species (see Figure 1). The proposed kinetics predict that when cyclooctene is present approximately ~1% of the porphyrin will be present as iron(IV) species; approximately 10% of the porphyrin is expected to be present as iron(IV) species when cyclooctene is absent. Iron (IV) species can be identified by peaks at 410 and 540 nm in the UV−visible spectroscopy.[71] As seen in Figure 8a, there is no significant change in the shape of the UV−visible spectrum taken at different reaction times when cyclooctene is present. The decrease in the intensity of the spectra as a function of time is due to porphyrin degradation. However, as shown in Figure 8b, a shoulder near 410 nm appears on the Soret peak when cyclooctene is absent. In addition, as shown in the inset of Figure 8b, there is a small increase in the absorbance near 540 nm after the addition of hydrogen peroxide. As predicted by the model of the reaction kinetics, iron(III) species predominate but there is an observable contribution to the UV−visible spectra from iron(IV) species in the absence of cyclooctene.

Effects of Substrate Concentration. The substrate concentration was varied to determine the ratio of the rate constants for reactions 6 and 7 (see Figure 1). As seen in Figure 9, the final yield is independent of the substrate concentration above about 0.4 M, indicating that reaction 6 does not compete with reaction 7 at high substrate concentrations. The ratio k_6/k_7 was determined by fitting the predicted to the observed variation in the yield of cyclooctene epoxide as a function of the concentration of cyclooctene. As seen in Figure 9, an excellent fit is achieved for a value of $k_6/k_7 = 0.6$.

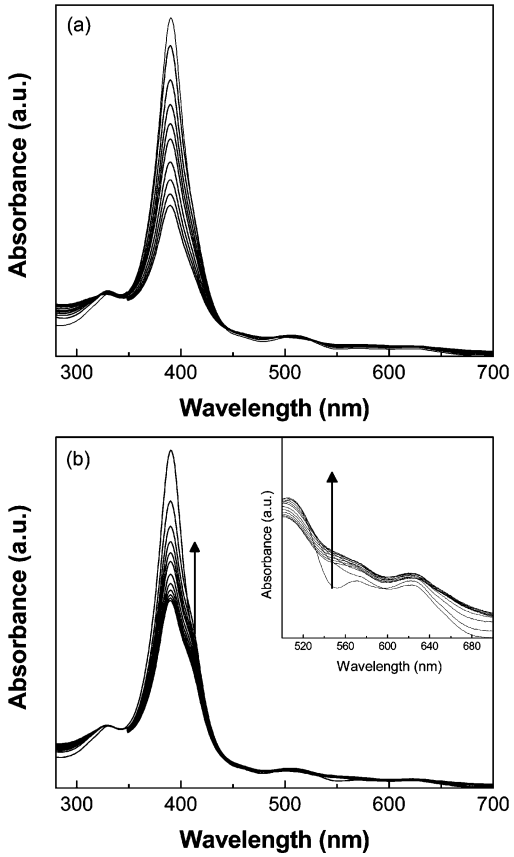

Figure 8. In situ UV−visible spectra taken as a function of time: (a) with cyclooctene present and (b) without cyclooctene present. The initial concentrations of porphyrin, peroxide, and cyclooctene were 15 μM, 2.5 mM, and 0.14 M, respectively.

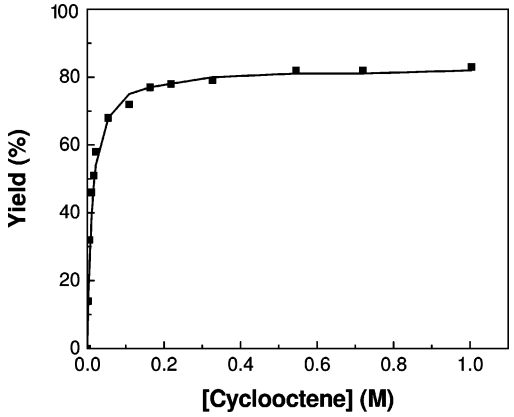

Figure 9. The yield of cyclooctene epoxide as a function of cyclooctene concentration. The concentration of H_2O_2 and porphyrin were 14.7 mM and 150 μM, respectively, for all experiments. The data points are for epoxide yield determined by gas chromatography, and the solid line represents the yield predicted by the proposed model.

Heterolytic Cleavage of the O−O Bond of Coordinated H_2O_2. Nam and co-workers have presented convincing evidence that heterolytic cleavage of the O−O bond in coordinated H_2O_2 occurs during the epoxidation of cy-

(71) Lee, K. A.; Nam, W. *Bull. Korean Chem. Soc.* **1996**, *17*, 669−671.

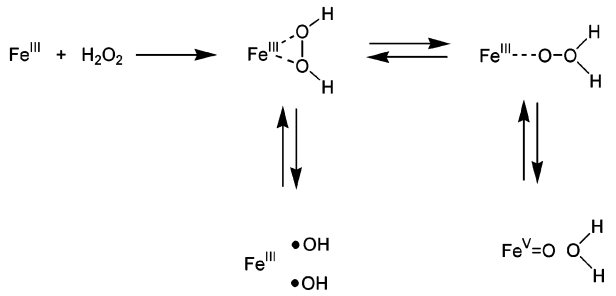

Figure 10. Mechanism suggested by Sawyer and co-workers for the activation of H_2O_2 by Fe^{3+} in acetonitrile.

clooctene by hydrogen peroxide in acetonitrile catalyzed by $(F_{20}TPP)Fe(OTf)$.[60] Two scenarios can be envisioned to explain how a hydrogen atom is transferred from the proximal to the distal oxygen of coordinated H_2O_2 either during or prior to heterolytic cleavage of the O−O bond in an aprotic solvent. The first explanation is that proton transfer is facilitated by some species in the reaction mixture. While water and hydrogen peroxide are obvious candidates for this role, we have shown above that water deactivates the catalyst rather than promoting catalytic activity and that the observed kinetics are independent of the hydrogen peroxide concentration. Experiments in which the concentration of free triflate was varied by the addition of silver triflate also did not affect the observed kinetics or final yield, indicating that triflate anions do not affect the cleavage of hydrogen peroxide.

The second possibility is that the hydrogen is transferred intramolecularly within the coordinated H_2O_2. Although such a scheme has not been proposed previously for porphyrins, Sawyer and co-workers have proposed such a process for iron salts dissolved in acetonitrile.[72−76] $FeCl_3$ was hypothesized to form a Lewis acid-Lewis base adduct equilibrated between a side-on and end-on form of the iron-hydrogen peroxide intermediate, as shown in Figure 10, inducing either a biradical (homolytic cleavage) or an oxene (heterolytic cleavage) character to the coordinated peroxide molecule.[73−75] Sawyer and co-workers later proposed that the oxene-like intermediate leads to the formation of an iron(V) oxo species which exhibits chemical characteristics and reactivities similar to those of iron(IV) pi-radical cation porphyrin species found in nature.[72] We suggest that a similar mechanism may account for the heterolytic cleavage of the O−O bond in H_2O_2 coordinated to $(F_{20}TPP)Fe^+$ in acetonitrile and that the iron(IV) hydroxo species may be formed via homolytic cleavage of the biradical species followed by a radical rebound step.

Role of Methanol Addition. The finding that water coordinated to the iron(III) porphyrin cation makes this species catalytically inactive raises the question as to whether this phenomenon affected any of our previous work in which a solvent system containing a mixture of alcohol and

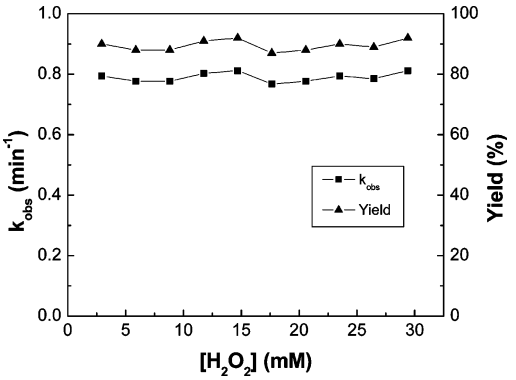

Figure 11. The effect of $[H_2O_2]$ on k_{obs} and epoxide yield in a (1:1) mixture of acetonitrile and methanol. Porphyrin and substrate concentrations were 75 μM and 0.72 M for all experiments.

acetonitrile was used.[64,65] To investigate the effect of water in the presence of methanol, $(F_{20}TPP)Fe(OTf)$ was dissolved in a 1:1 mixture of acetonitrile and methanol. As shown in Figure 11, neither Y_∞ nor k_{obs} are affected by the initial concentration of H_2O_2 (i.e., the water content) added to the reaction mixture; this in complete agreement with our earlier observations.[64,65]

The extent of methanol coordination was investigated using UV−visible spectroscopy. The addition of microliter aliquots of methanol to a 15 μM solution of $(F_{20}TPP)Fe(OTf)$ dissolved in acetonitrile caused a shift in the position of the Soret peak from 390 to 388 nm. This shift occurred at low methanol concentrations, and complete conversion to the methanol-coordinated species was evidenced by no further change in the spectrum for methanol concentrations above ~1 vol %. This observation suggests that the equilibrium constant for coordination of methanol to the iron(III) porphyrin cation is of the same order of magnitude as that found for coordination by water. Thus, when methanol is present in large excess relative to water, methanol will displace all of the water present in the coordination sphere of the iron(III) porphyrin cation. Coordination of methanol to the iron(III) porphyrin cation was also verified by ^{1}H NMR spectroscopy, as indicated by a shift in the β-pyrrole resonance from 60 to 65 ppm[66] upon the addition of methanol.

Comparison of Protic and Aprotic Solvent Systems. As shown here and in our previous work,[64−66] the mechanism for $(F_{20}TPP)Fe$-catalyzed epoxidation of cyclooctene by hydrogen peroxide is similar for both aprotic and protic solvent systems. For homolytic cleavage of the O−O bond in coordinated H_2O_2, the value of k_4K_2 is smaller in methanol than in acetonitrile, 5 s^{-1} M^{-1} versus 9 s^{-1} M^{-1}. And for heterolytic cleavage of the O−O bond, the value of $k_3K_2[CH_3OH] = 13\ [CH_3OH]\ M^{-1}\ s^{-1}$, which for pure methanol gives a value of 290 M^{-1} s^{-1}, whereas $k_3K_2 = 86\ M^{-1}\ s^{-1}$ for an acetonitrile solution. The faster rate of heterolytic cleavage and slower rate of homolytic cleavage for the protic system results in a value of Y_∞ as high as 96%, while Y_∞ is only 83% in the aprotic system. The iron(IV) pi-radical cations also exhibit a higher reactivity toward cyclooctene relative to H_2O_2 in protic versus aprotic solvents ($k_6/k_7 = 0.30$ vs 0.60). By contrast, though, the reactivity of iron(IV) hydroxo

(72) Tung, H. C.; Kang, C.; Sawyer, D. T. *J. Am. Chem. Soc.* **1992**, *114*, 3445−3455.
(73) Sugimoto, H.; Sawyer, D. T. *J. Org. Chem.* **1985**, *50*, 1784−1786.
(74) Sawyer, D. T. *CHEMTECH* **1988**, 369−375.
(75) Strukul, G. *Catalytic Oxidations with Hydrogen Peroxide as Oxidant*; Kluwer Academic Publishers: Boston, MA, 1992.
(76) Bruice, T. C. *Acc. Chem. Res.* **1991**, *24*, 243−249.

cations is not affected by the nature of the solvent (k_5 = 225 M^{-1} s^{-1} for both systems). Finally, a greater extent of porphyrin degradation is observed for the aprotic solvent system than for the protic solvent system. This relationship is consistent with the observation of a higher value of k_4K_2 for the aprotic solvent system, since porphyrin degradation is believed to result from the attack of free radicals (e.g., $OH^{\bullet}$) on the porphyrin ring, which are produced via reactions 4 and 6.[64,65,70] Decreased porphyrin degradation in methanol may also result from scavenging of the hydroxyl radical by methanol.

Experiments were also conducted to study the kinetics of the triflate-coordinated species in methanol (20 M). Under these conditions, the observed rate constant was 1.02 min^{-1}, and the yield of epoxide was 96%. It is believed that in this case the catalyst operates according to the same mechanism as that proposed previously for (F_{20}TPP)FeCl dissolved in methanol and that, independent of the initial porphyrin salt used, $[(F_{20}TPP)Fe(CH_3OH)]^+$ is the precursor to the pi-radical cation species. In support of this hypothesis, the value of k_{obs} was determined to be 1.02 min^{-1}, and Y_∞ was determined to be 96%, corresponding to values of k_3K_2 = 11 [MeOH] M^{-1} s^{-1} and k_4K_2 = 5 M^{-1} s^{-1} for (F_{20}TPP)-Fe(OTf) dissolved in 20 M methanol. The corresponding values are k_3K_2 = 13 [MeOH] M^{-1} s^{-1} and k_4K_2 = 5 M^{-1} s^{-1} for (F_{20}TPP)FeCl dissolved in methanol.[10]

Conclusions

A mechanism has been presented for (F_{20}TPP)Fe(OTf)-catalyzed epoxidation of cyclooctene in acetonitrile using hydrogen peroxide as the oxidant and has been shown to be consistent with all experimental evidence. This mechanism is similar to that presented for (F_{20}TPP)FeCl in the presence of a protic solvent.[64,65] In both systems, only iron(III) porphyrin species that are not coordinated by a strongly bound axial ligand are catalytically active. The main difference between the two solvent systems is that the mechanism for cleavage of the oxygen−oxygen bond of coordinated hydrogen peroxide appears to be intramolecular in an aprotic solvent and acid-catalyzed in protic solvent. The rate parameters obtained in this study of iron porphyrin-catalyzed reaction occurring in an aprotic solvent can be compared directly with the rate parameters for the same reaction occurring in a protic solvent. In an aprotic solvent, hydrogen peroxide is used less efficiently for epoxidation of cyclooctene than in a protic solvent, and porphyrin degradation occurs much more rapidly than in a protic solvent. The higher rates of hydrogen peroxide decomposition and porphyrin degradation are both a consequence of the higher rate of free radical generation via homolytic cleavage of coordinated H_2O_2 occurring in an aprotic solvent. It was also observed that water can deactivate the catalyst in aprotic solvent by coordinating to the iron porphyrin. Since water can be displaced from the coordination sphere of the iron(III) porphyrin by methanol, the water present in a hydrogen peroxide solution does not affect the catalytic activity of (F_{20}-TPP)Fe^+ dissolved in methanol. This is a significant finding, suggesting that future studies of iron porphyrins in aprotic solvents can be affected by small amounts of water.

Acknowledgment. This work was supported by the Director, Office of Basic Energy Sciences, Chemical Sciences Division of the U.S. Department of Energy under Contract DE-AC02-05CH11231.

IC060757C